Detailed Northern Anatolian Fault Zone crustal structure from receiver functions

Cornwell, D.G.[1,*], Kahraman, M.[2], Thompson, D.A.[3], Rost, S.[3], Houseman, G.A.[3], Turkelli, N.[2], Teoman, U.[2], Poyraz, S.A.[2], Gülen, L.[4], and Utkucu, M.[4]

[1] School of Geosciences, University of Aberdeen, Aberdeen, AB25 3UE, U.K.; [2] Kandilli Observatory & Earthquake Research Institute, Bogazic Universitesi, Istanbul, Turkey; [3] School of Earth & Environment, University of Leeds, Leeds, LS2 9JT, U.K.; [4] Department of Geophysical Engineering, Sakarya Universitesi, Turkey. * d.cornwell@abdn.ac.uk

T23E-2633

faultlab.leeds.ac.uk

1. INTRODUCTION

The Northern Anatolian Fault Zone (NAFZ) is a major continental strike-slip fault system that is the main focus of deformation (~20-30 mm/yr) in northern Anatolia, Turkey. Twelve large (M>6.7) earthquakes occurred along the NAFZ since 1939 and their westward progression poses a future seismic hazard to Istanbul.

The Faultlab experiment aims to understand how the lower crust affects the re-occurrence of earthquakes along the NAFZ by developing a crustal scale model that is consistent with cumulative strain derived from surface geology and geodetic measurements.

We show high resolution crustal structure by interpreting teleseismic receiver functions recorded by a recent (May 2012-Sept. 2013) rectangular seismometer array spanning the NAFZ with 66 stations at ~7 km inter-station spacing and 7 additional stations further afield (Fig. 1).

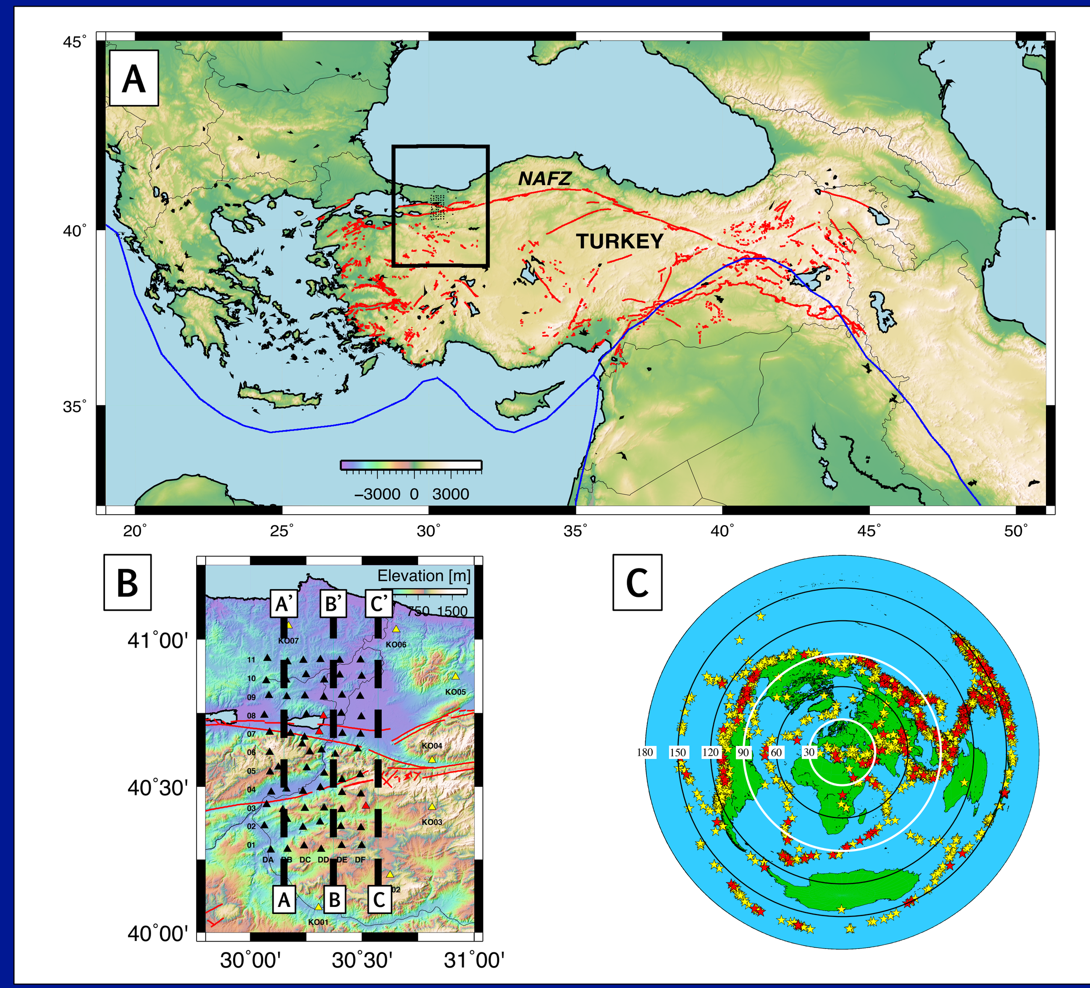

Fig. 1: A) Regional map of the study area (rectangle) with NUVEL-1 plate boundaries (blue) and Turkey faults. B) Topographical map of the study region with the locations of temporary (black/yellow) and permanent (red) seismological stations. C) Magnitude >5.5 earthquake locations during the DANA deployment (red stars) and permanent station data since 2009 (yellow stars).

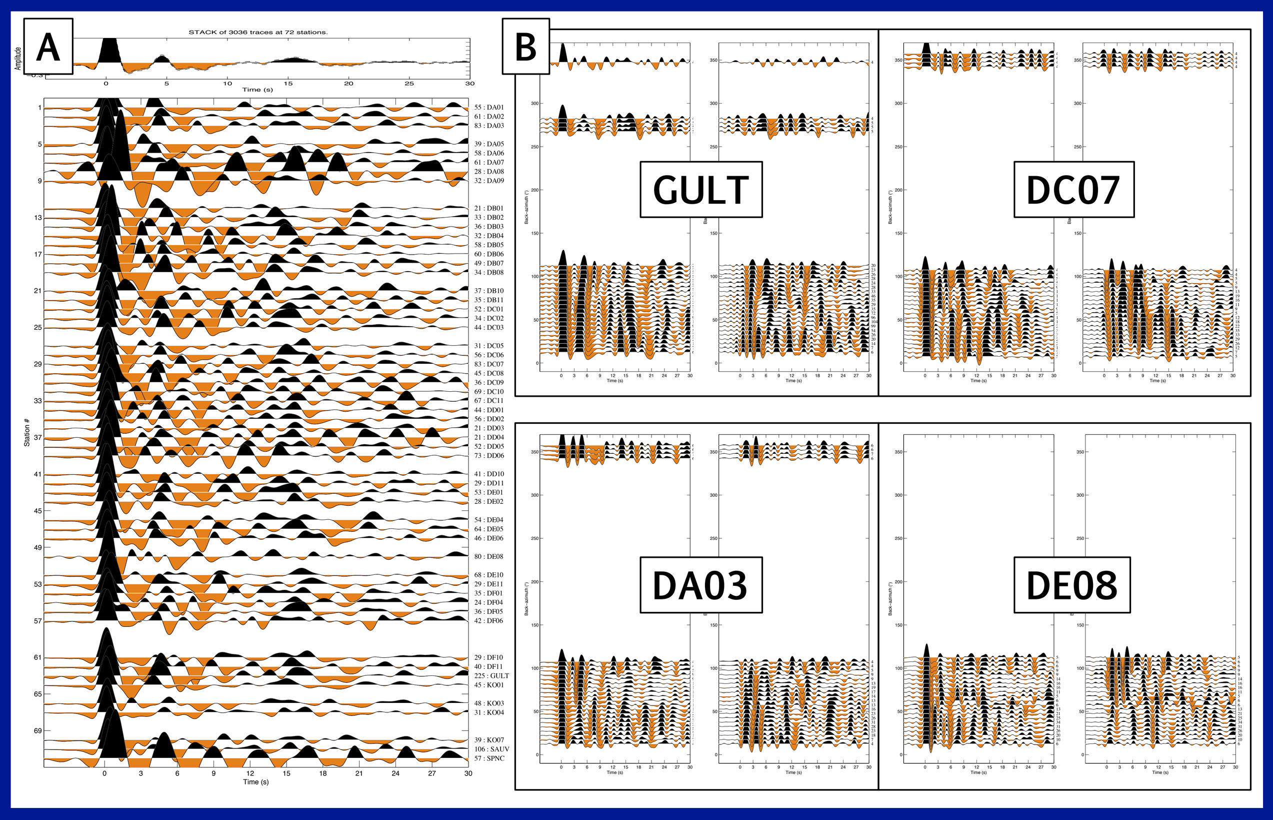

Fig. 2: A) All and station ETMTRF receiver function stacks (if N>20). B) Back-azimuth stacks of radial (*P-SV* conversions) & transverse (*P-SH*) component receiver functions at example stations (Fig. 1).

2. RECEIVER FUNCTION DATA

Receiver functions (RFs) were calculated with the extended time multi-taper (ETMTRF, Helffrich, 2006) methods (F_{MAX}=1 Hz) using M>5.5 events (Fig. 1C). 3043 high-quality RFs were selected for further analyses. Back-azimuthal coverage is excellent from north to east but sparse elsewhere.

RF stacks (Fig. 2) show clear Moho *P-S* and multiple energy for most stations. High amplitude transverse RF energy (caused by anisotropy or dipping layers) occurs at *P-S* delay times corresponding to the upper crust, lower crust and upper mantle with consistent phase polarity reversals at ~N060E°.

3. H-κ STACKING

Crustal thickness and bulk crustal V_P/V_S were constrained across the NAFZ by applying single station H-κ stacking (Zhu & Kanamori, 2000) to RFs:

- We find crustal thicknesses and V_P/V_S ratios of 31-35 km and 1.76-1.84, respectively.
- Previous refraction (Bekler et al., 2008) and RF studies (Vanacore, et. al., 2013) found 32-35 and 34-36 km thick crust in our study region.
- Poisson's ratios of 0.26-0.29 are consistent with Sakarya and Istanbul Zone metamorphic crust.
- Preliminary results do not show evidence for a Moho beneath either of the NAFZ fault strands.

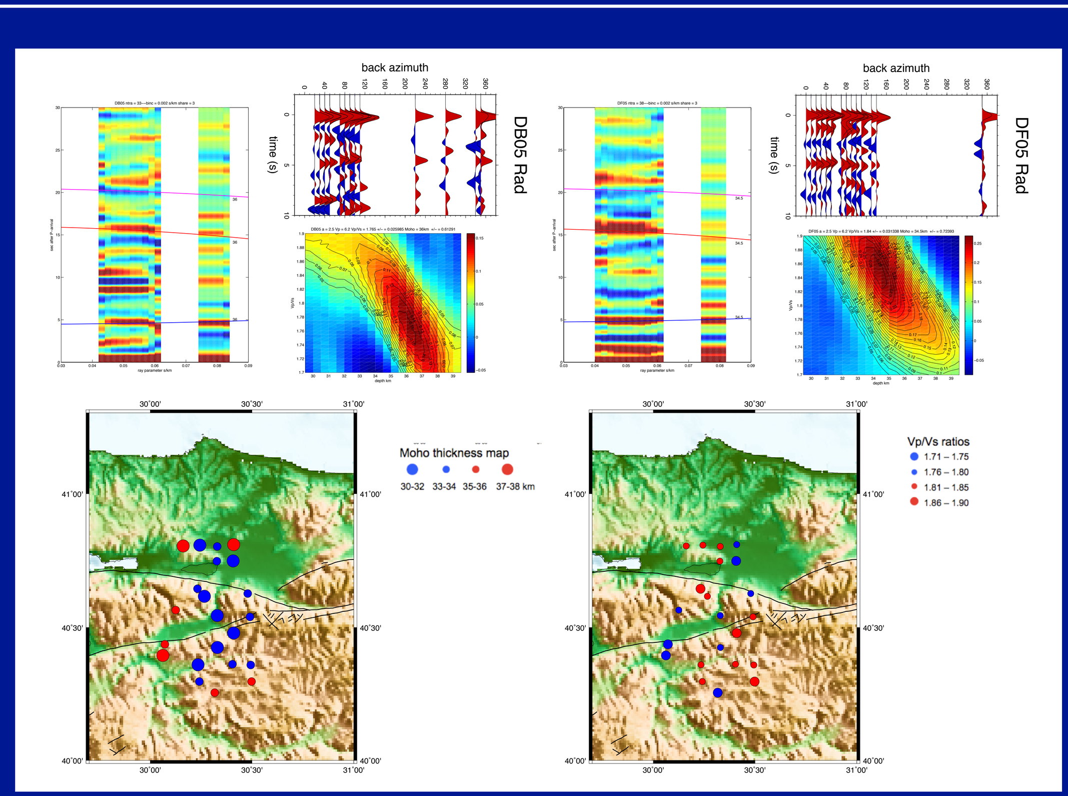

Fig. 3: H-κ stacking result examples (upper panels) and summary maps showing preliminary crustal thickness and whole crust V_P/V_S (lower panels).

4. COMMON CONVERSION POINT RECEIVER FUNCTION MIGRATION

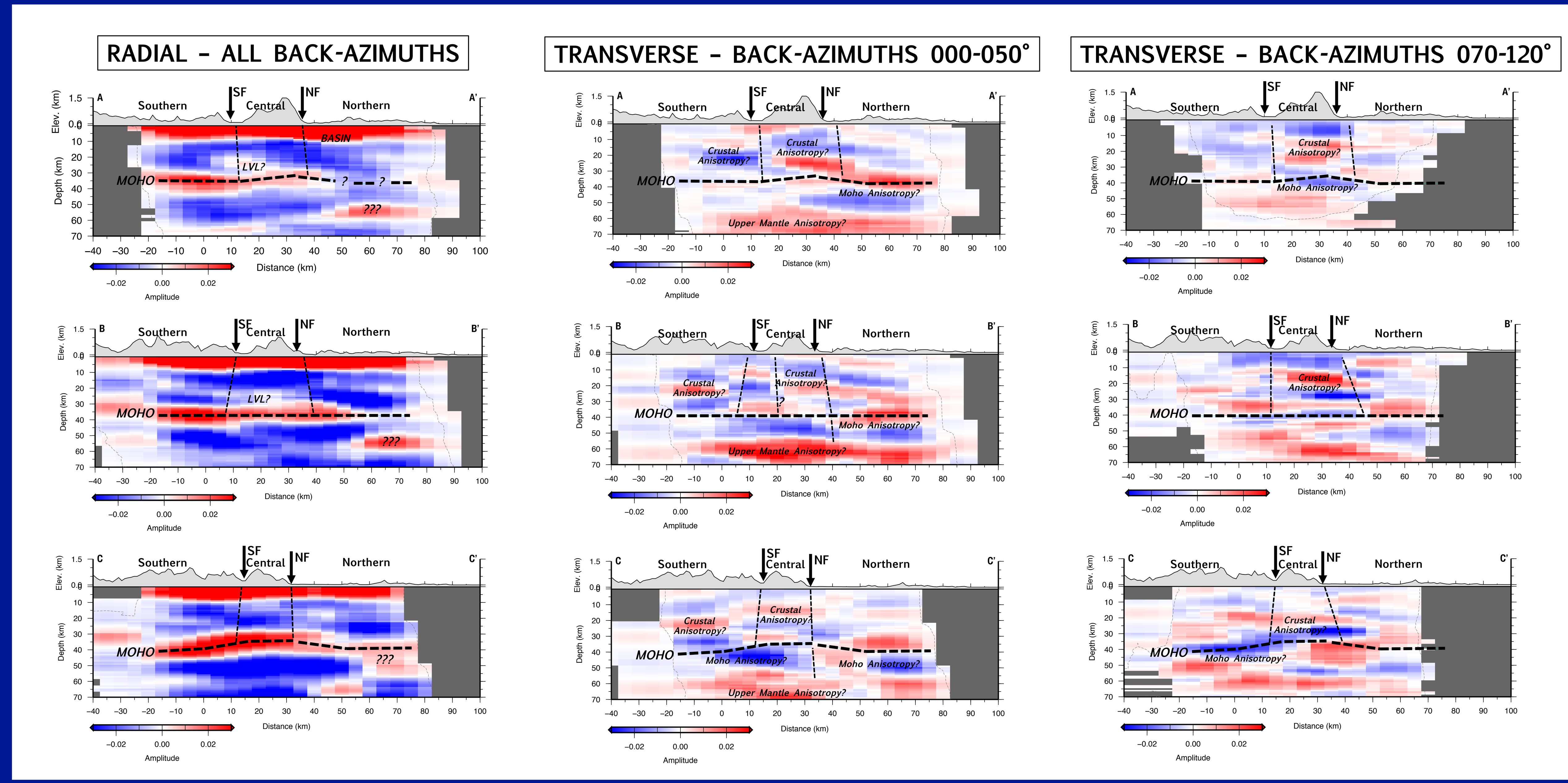

Fig. 4: Common conversion point (CCP) migrated 1 Hz ETMTRF receiver functions along three south-north profiles (see Fig. 1) that span the southern (SF) and northern (NF) branches of the NAFZ. RFs were back-projected along their raypaths using the IASP91 velocity model, summed into 5x5x1 km voxels then horizontally smoothed over 20 km. Subsets of the full dataset were used for the transverse profiles according to event back-azimuth. Labels derived from the radial profiles are copied onto the transverse profiles for comparison. SRTM topography is plotted above each profile and LVL=low-velocity layer.

5. PRELIMINARY INTERPRETATION

- Abrupt first-order changes in upper and lower crustal structure occur beneath the surface locations of the two NAFZ branches.
- A clear Moho is imaged beneath the southern (35-39 km depth) and central (~35 km depth) crustal blocks cut by the NAFZ.
- The northern block is underlain by a low amplitude Moho conversion underlain by a high amplitude conversion at 50-60 km.
- Large amplitude transverse energy indicates anisotropic crust and/or dipping layer effects that vary south to north, being strongest beneath the central crustal block.
- There is evidence for upper mantle anisotropy that is strongest beneath the central NAFZ and changes in character beneath the northern NAFZ branch.

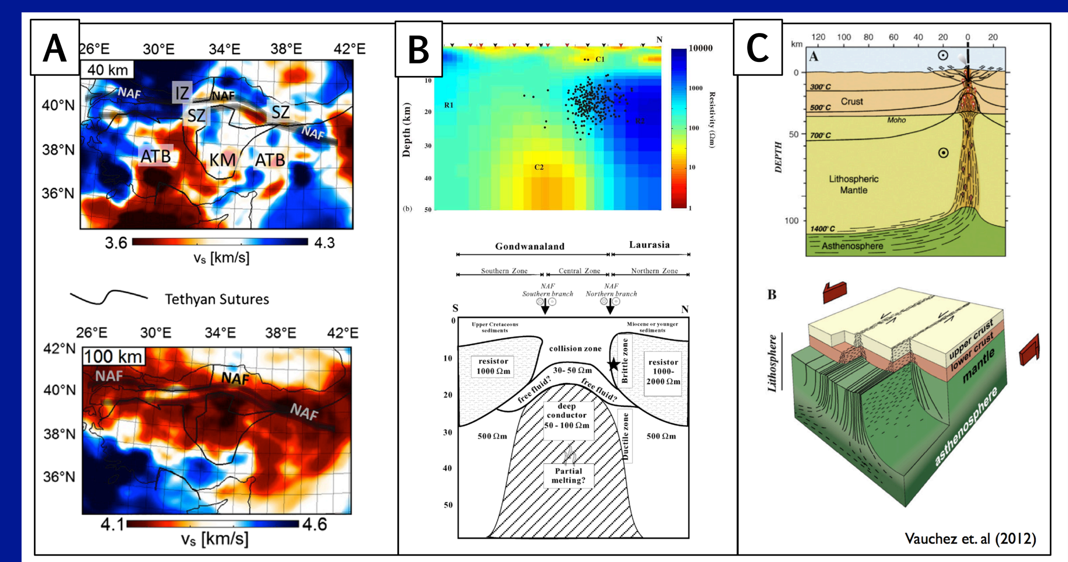

Fig. 5: A) Depth slices from the *S*-wave tomography model of Fichtner *et al.*, (2013) at 40 and 100 km. B) Crustal conductivity profile and interpretation from an MT study (Tank *et al.*, 2005). C) Strike-slip fault zone schematic diagrams (Vauchez et *al.*, 2012).

- Upper mantle anisotropy may be further evidence of partial melt
- Three contrasting abutting crustal blocks is consistent with crustal conductivity variations
- Current NAFZ models do not include crustal heterogeneity

7. ACKNOWLEDGEMENTS

Faultlab is a Natural Environmental Research Council (NERC) sponsored project that uses SEIS-UK (NERC Geophysical Equipment Pool) seismometer equipment. We thank Victoria Lane and David Hawthorn of SEIS-UK, Hannah Bentham, Dan Frost, Oğuz Göğüş, Ekbal Hussain, Luke Jackson, Sandra Karl, Liz Vanacore and Tadashi Yamasaki for fieldwork help.

8. REFERENCES

- Bekler, T. and Gurbuz, C., (2008) Insight into the crustal structure of the eastern Marmara region, NW Turkey, Pure Appl. Geophys., 165, 295-309.
- Fichtner, A., et al., (2013) The deep structure of the North Anatolian Fault Zone. Earth and Planetary Science Letters, http://dx.doi.org/10.1016/j.epsl.2013.04.027i
- Helffrich, G., (2006) Extended multi-taper frequency domain cross-correlation receiver function estimation, BSSA, 96(1), doi:10.1785/0120050098
- Tank, S. B., et al., (2005) Magnetotelluric imaging of the fault rupture area of the 1999 Izmit (Turkey) earthquake, Phys. Earth Planet. Int., 150, 213-225.
- Vanacore, E., et al., (2013). Moho structure of the Anatolian plate from receiver function analysis. Geophys. J. Int. 193, http://dx.doi.org/10.1093/gji/ggs107.
- Vauchez, A. et al., (2012) Faults (shear zones) in the Earth's mantle, Tectonophysics, doi:10.1016/j.tecto.2012.06.006
- Zhu, L. and Kanamori, H. (2000) Moho depth variation in southern California from teleseismic receiver functions, J. Geophys. Res., 105, 2969-2980.